PHYSICAL REVIEW B **82**, 201311(R) (2010)

Phonon-induced resistance oscillations of two-dimensional electron systems drifting with supersonic velocities

I. A. Dmitriev,[1,*] R. Gellmann,[2,†] and M. G. Vavilov[3]
[1]*Institut für Nanotechnologie, Karlsruher Institut für Technologie, 76021 Karlsruhe, Germany*
[2]*Inst. für Theorie der Kondensierten Materie, Karlsruher Institut für Technologie, 76128 Karlsruhe, Germany*
[3]*Department of Physics, University of Wisconsin, Madison, Wisconsin 53706, USA*
(Received 7 October 2010; published 17 November 2010)

We present a theory of the phonon-assisted nonlinear dc transport of two-dimensional electrons in high Landau levels. The nonlinear dissipative resistivity displays quantum magneto-oscillations governed by two parameters which are proportional to the Hall drift velocity v_H of electrons in electric field and the speed of sound s. In the subsonic regime, $v_H<s$, the theory quantitatively reproduces the oscillation pattern observed in recent experiments. We also find the $\pi/2$ phase change in oscillations across the sound barrier $v_H=s$. In the supersonic regime, $v_H>s$, the amplitude of oscillations saturates with lowering temperature while the subsonic region displays exponential suppression of the phonon-assisted oscillations with temperature.

DOI: 10.1103/PhysRevB.82.201311 PACS number(s): 73.40.−c, 73.21.−b, 73.43.−f

A high-mobility two-dimensional electron gas (2DEG) in a weakly quantizing perpendicular magnetic field B displays a rich variety of magneto-oscillation phenomena. These phenomena are defined by the ratio of energy parameters and the Landau-level spacing $\hbar\omega_c$ with $\omega_c=eB/mc$ or by ratio of the spatial length scales and the cyclotron radius $R_c=v_F/\omega_c$, where $v_F(p_F=mv_F)$ is the Fermi velocity (momentum).

Examples of magneto-oscillations include: (i) the microwave-induced resistance oscillations (MIRO) (Refs. 1–3) and associated zero-resistance states,[4,5] controlled by the ratio of the the microwave frequency ω and cyclotron frequency ω_c, $\epsilon_{ac}\equiv\omega/\omega_c$; (ii) the Hall field-induced resistance oscillations (HIRO) (Refs. 6 and 7) and associated zero-differential resistance states,[8] in the dc electric field E, governed by $\epsilon_{dc}\equiv eE(2R_c)/\hbar\omega_c$; (iii) the phonon-induced resistance oscillations (PIRO),[9–12] characterized by the ratio $\epsilon_{ph}\equiv\omega_\pi/\omega_c$, where $\hbar\omega_\pi=2sp_F$ is the energy of an acoustic phonon with momentum $2p_F$ and s is the speed of sound. The above oscillations stem from commensurability of energy change in photon (MIRO); disorder (HIRO), and phonon-assisted (PIRO) scattering events and the $\hbar\omega_c$-periodic oscillations of the density of states (DoS). MIRO and HIRO,[1,2,4–8] as well as their interplay,[13–15] have been studied in detail over the past decade.

In this Rapid Communication, we present a theory of a phonon-assisted transport in strong dc electric fields. In the nonlinear dc response, our results are consistent with the observed evolution of PIRO in the regime $\epsilon_{dc}<\epsilon_{ph}$ in recent experiment.[10] We predict that the phase of oscillations changes across the sound barrier $\epsilon_{dc}=\epsilon_{ph}$, where the Hall drift velocity $v_H=cE/B$ equals to the speed of sound. We also analyze the temperature dependence of the phonon-assisted transport in different regimes.

For a 2DEG in a region of classically strong B, when ω_c exceeds the transport scattering rate $1/\tau_{tr}$, the dissipative current j_x is conveniently expressed in terms of scattering rates $\Pi_{x_1\to x_2}$ which represent the semiclassical probability of the corresponding shift of the guiding center of the cyclotron orbit due to scattering,[14,16]

$$j_x=2\nu_0 e\int_{-\infty}^{0}dx_1\int_{0}^{\infty}dx_2(\Pi_{x_1\to x_2}-\Pi_{x_2\to x_1}),$$

$$\Pi_{x_1\to x_2}=\int P_{\varphi,\varphi'}(\varepsilon)\delta(x_1-x_2+\boldsymbol{e}_x\Delta\boldsymbol{R}_{\varphi,\varphi'})d\varepsilon\frac{d\varphi d\varphi'}{4\pi^2}, \quad (1)$$

where $\nu_0=m/2\pi$ is the DoS at $B=0$ (hereafter $\hbar=1$). For $v_F\gg v_H,s$, the displacement of the guiding center along the electric field $\boldsymbol{E}=E\boldsymbol{e}_x$ is $\boldsymbol{e}_x\Delta\boldsymbol{R}_{\varphi,\varphi'}=R_c(\sin\varphi-\sin\varphi')$ for the change in the momentum direction from φ to φ' [see Fig. 1(f)]. The Einstein transition rates are

$$P_{\varphi,\varphi'}(\varepsilon)=\tau^{-1}_{\varphi-\varphi'}\mathcal{M}(\varepsilon,\varepsilon+W_{\varphi,\varphi'})+\frac{g^2|\omega_{\varphi-\varphi'}|}{2}N_{\omega_{\varphi-\varphi'}}\times\mathcal{M}(\varepsilon,\varepsilon+W_{\varphi,\varphi'}+|\omega_{\varphi-\varphi'}|)+\frac{g^2|\omega_{\varphi-\varphi'}|}{2}\times(N_{\omega_{\varphi-\varphi'}}+1)\mathcal{M}(\varepsilon,\varepsilon+W_{\varphi,\varphi'}-|\omega_{\varphi-\varphi'}|). \quad (2)$$

The first line in Eq. (2) represents the scattering off static disorder studied in Refs. 7 and 14. Here, the electron kinetic energy ε changes by the electrostatic work $W_{\varphi,\varphi'}=e\boldsymbol{E}\Delta\boldsymbol{R}_{\varphi,\varphi'}$. The second (third) line in Eq. (2) describes processes with absorption (emission) of a phonon with energy $|\omega_{\varphi-\varphi'}|$, where $\omega_{\varphi-\varphi'}=2p_Fs\sin(\varphi-\varphi')/2$ for $s\ll v_F$. The Planck's function $N_\omega=1/[\exp(|\omega|/T)-1]$ accounts for the thermal occupation of phonon modes and g is the dimensionless electron-phonon coupling constant.[17]

Factors $\mathcal{M}(\varepsilon,\varepsilon')=\tilde{\nu}(\varepsilon)\tilde{\nu}(\varepsilon')f(\varepsilon)[1-f(\varepsilon')]$ in Eq. (2) contain the Fermi function $f(\varepsilon)=1/\{\exp[(\varepsilon-\mu)/T]+1\}$ and the product of the DoS of initial and final states. The DoS in the experimentally relevant region of weak magnetic fields, $\tau_q\omega_c\lesssim 1$, has the form

$$\tilde{\nu}(\varepsilon)\equiv\nu(\varepsilon)/\nu_0=1-2\lambda\cos(2\pi\varepsilon/\omega_c), \quad (3)$$

where $\lambda=\exp(-\pi/\omega_c\tau_q)$ and τ_q is the quantum scattering time off disorder.

Using Eqs. (1)–(3) and assuming $T\tau_q\gtrsim 1$, we obtain

$$j_x=\frac{\rho_D E\tau_{tr}}{\rho_H^2}(\Gamma_{dis}+\Gamma_{ph}^{(sm)}+\Gamma_{ph}^{(osc)}), \quad (4)$$

where $\rho_D=\pi\nu_0/(e^2N_e\tau_{tr})$ and $\rho_H=B/(ecN_e)$ are the Drude and Hall resistivities, $N_e=mv_F^2\nu_0$ is the electron surface den-

 ©2010 The American Physical Society

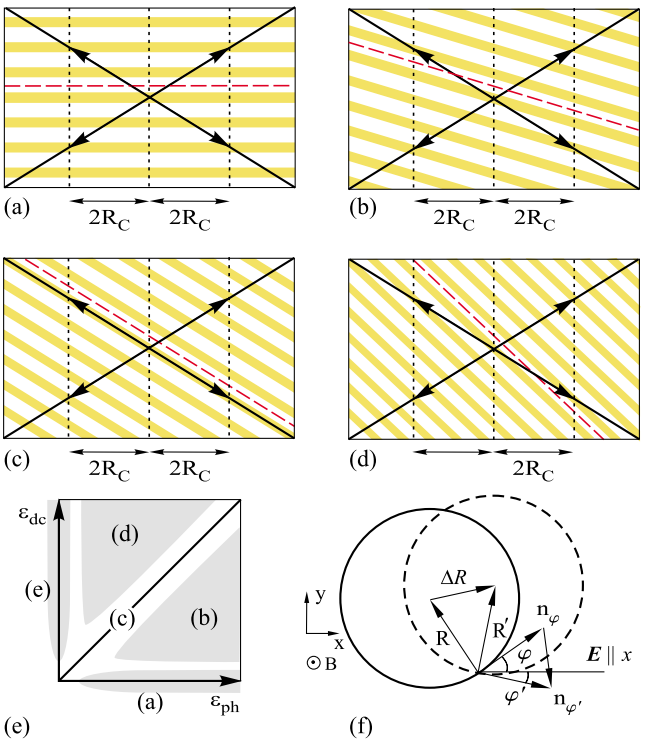

FIG. 1. (Color online) Illustration of electron-phonon-scattering processes in different regimes: (a) for $\epsilon_{dc}=0$; (b) for $\epsilon_{dc}<\epsilon_{ph}$; (c) for $\epsilon_{dc}=\epsilon_{ph}$; and (d) for $\epsilon_{dc}>\epsilon_{ph}$. Arrows show the change in the total energy of electron due to emission or absorption of a $2p_F$ phonon accompanied by the shift of the guiding center of the cyclotron orbit by $2R_C$ along or against the dc field. The arrows are directed along the sound cone (solid lines) while the strength of dc field determines the tilt of Landau levels [maxima of oscillatory DoS, Eq. (3), are marked by yellow stripes]. Dashed line marks the position of the Fermi level. The position of four regions Figs. 1(a)–1(d) in the $\epsilon_{ph}-\epsilon_{dc}$ plane is shown in Fig. 1(e). Figure 1(f) illustrates the real-space shift ΔR of the cyclotron guiding center and the change in the electron momentum for scattering from φ to φ'.

sity. The effective scattering rate of disorder was obtained in Ref. 7: $\Gamma_{dis}(\epsilon_{dc})=\tau_{tr}^{-1}-2\lambda^2F''(\pi\epsilon_{dc})$ with $F(x)=\Sigma J_n^2(x)/\tau_n$ and $J_n(x)$ standing for the Bessel functions; the scattering rate $\tau_{\varphi-\varphi'}^{-1}=\Sigma\tau_n^{-1}e^{in(\varphi-\varphi')}$ is presented by its angular harmonics $1/\tau_n$ ($\tau_0\equiv\tau_q$).

Here we focus on the phonon-assisted scattering rates

$$\begin{Bmatrix}\Gamma_{ph}^{(sm)}\\ \Gamma_{ph}^{(osc)}\end{Bmatrix}=g^2T\int\begin{Bmatrix}1\\ 2\lambda^2\cos\dfrac{W_{\varphi,\varphi'}-\omega_{\varphi-\varphi'}}{\omega_c/2\pi}\end{Bmatrix}\times(\sin\varphi-\sin\varphi')^2\Lambda\left(\frac{\omega_{\varphi-\varphi'}}{2T},\frac{W_{\varphi,\varphi'}}{2T}\right)\frac{d\varphi d\varphi'}{4\pi^2},\tag{5}$$

where $\Gamma_{ph}^{(sm)}(\epsilon_{dc},\epsilon_{ph})$ and $\Gamma_{ph}^{(osc)}(\epsilon_{dc},\epsilon_{ph})$ denote the smooth and oscillatory components of the electron-phonon-scattering rate and $\Lambda(x,y)=S(x)S(x-y)/S(y)$ is written in terms of $S(x)\equiv x/\sinh x$. We first study the behavior of $\Gamma_{ph}^{(sm)}$ and $\Gamma_{ph}^{(osc)}$ in the experimentally relevant limit $T\gg\omega_c$ and then analyze how these rates evolve with lowering T.

At high $T\gtrsim W,\omega$, we approximate $\Lambda(\omega/2T,W/2T)\approx1$ in Eq. (5) and obtain constant $\Gamma_{ph}^{(sm)}=g^2T$ for the smooth part of electron-phonon transport scattering rate. The oscillatory part, which represents the effect of the Landau quantization, reduces to

$$\Gamma_{ph}^{(osc)}=8\lambda^2g^2T\int_0^{2\pi}\frac{d\varphi_+d\varphi_-}{4\pi^2}\sin^2\varphi_-\cos^2\varphi_+\times\cos[2\pi\sin\varphi_-(\epsilon_{ph}-\epsilon_{dc}\cos\varphi_+)].\tag{6}$$

The behavior of $\Gamma_{ph}^{(osc)}(\epsilon_{dc},\epsilon_{ph})$ is different in parametric regimes, illustrated in Fig. 1(e). In the limit of weak electric fields, $\epsilon_{dc}\ll1$, the current is linear in the applied dc field and

$$\Gamma_{ph}^{(osc)}(0,\epsilon_{ph})=2\lambda^2g^2T[J_0(2\pi\epsilon_{ph})-J_2(2\pi\epsilon_{ph})].\tag{7}$$

The oscillations with $\epsilon_{ph}=\omega_\pi/\omega_c$ in Eq. (7) are driven by commensurability between the phonon energy $\omega_\pi=2p_Fs$ and the period of DoS oscillations ω_c, see Fig. 1(a). For $\epsilon_{ph}\gtrsim1$, Eq. (7) gives $\Gamma_{ph}^{(osc)}(0,\epsilon_{ph})=(4\lambda^2g^2T/\pi\sqrt{\epsilon_{ph}})\cos(2\pi\epsilon_{ph}-\pi/4)$. This regime was studied by Raichev.[18] The difference in the oscillations phase in Eq. (7) and Ref. 18 is due to a different choice of the phonon scattering form factor in narrow vs wide quantum wells.

A strong Hall field tilts the Landau levels and changes the commensurability conditions for electron-phonon scattering as shown in Figs. 1(b)–1(d), resulting in oscillations with combined parameters $\epsilon_\pm\equiv\epsilon_{dc}\pm\epsilon_{ph}$. Equivalently, this effect can be viewed as a result of the Doppler shift of the phonon modes in the frame moving with the Hall velocity v_H in y direction. In the moving frame, the electric field is absent while the phonon speed changes as $s\to s-v_H\cos\varphi_+$ in the argument of cosine in the second line of Eq. (6). The latter formulation is particularly useful in the case of complicated spectrum of phonons.

At $\epsilon_{dc}\gg1$, the rate $\Gamma_{ph}^{(osc)}$ can be approximated as

$$\Gamma_{ph}^{(osc)}(\epsilon_{dc},\epsilon_{ph})=-\frac{2}{\pi^2}\lambda^2g^2T\frac{\partial^2\Phi(\epsilon_{dc},\epsilon_{ph})}{\partial\epsilon_{dc}^2},$$

$$\Phi(\epsilon_{dc},\epsilon_{ph})=\frac{1}{\sqrt{\epsilon_{dc}}}\sum_\pm B_{\mathrm{sign}\,\epsilon_\pm}(|\epsilon_\pm|),$$

$$B_{\pm1}(z)=\sqrt{z/8}[J_{-1/4}^2(\pi z)\pm J_{1/4}^2(\pi z)].\tag{8}$$

This expression can be simplified in three cases when electron drifts with subsonic velocity [$v_H<s$ or $\epsilon_{dc}<\epsilon_{ph}$, Fig. 1(b)]; velocity of sound [$v_H=s$ or $\epsilon_{dc}=\epsilon_{ph}$, Fig. 1(c)]; and supersonic velocity [$v_H>s$ or $\epsilon_{dc}>\epsilon_{ph}$, Fig. 1(d)],

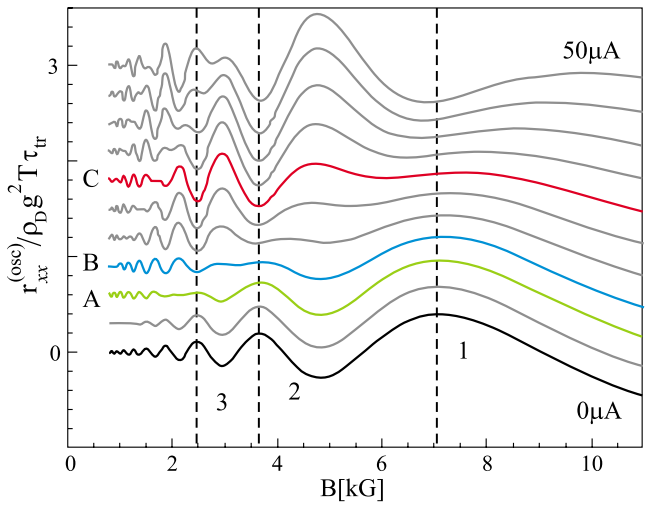

FIG. 2. (Color online) $r_{xx}^{(\mathrm{osc})}$ vs B for several values of current I varying from 0 to 50 μA in 5 μA steps. Traces are vertically offset for clarity. Traces (a) [10 μA], (b) [15 μA], and (c) [30 μA] correspond approximately to the values of I at which third, second, and first PIRO peaks disappear before evolving into minima at higher currents. Very similar values (a) [10 μA], (b) [14 μA], and (c) [28 μA] were found in the experiment (see Fig. 2 of Ref. 10).

$$\Gamma_{\mathrm{ph}}^{(\mathrm{osc})}(\epsilon_{\mathrm{dc}},\epsilon_{\mathrm{ph}}) = 4\lambda^2 g^2 T \times \begin{cases} \left(\dfrac{\sin 2\pi\epsilon_+}{\pi^2\sqrt{\epsilon_{\mathrm{dc}}\epsilon_+}} + \dfrac{\cos 2\pi\epsilon_-}{\pi^2\sqrt{\epsilon_{\mathrm{dc}}|\epsilon_-|}}\right), & \epsilon_{\mathrm{dc}} \ll \epsilon_{\mathrm{ph}}, \\ \left(\dfrac{1}{3\sqrt{\pi\epsilon_{\mathrm{dc}}}\Gamma^2(3/4)} + \dfrac{\sqrt{2}}{2\pi^2\epsilon_{\mathrm{dc}}}\right), & \epsilon_{\mathrm{dc}} = \epsilon_{\mathrm{ph}}, \\ \left(\dfrac{\sin 2\pi\epsilon_+}{\pi^2\sqrt{\epsilon_{\mathrm{dc}}\epsilon_+}} + \dfrac{\sin 2\pi\epsilon_-}{\pi^2\sqrt{\epsilon_{\mathrm{dc}}\epsilon_-}}\right), & \epsilon_{\mathrm{dc}} \gg \epsilon_{\mathrm{ph}}. \end{cases} \tag{9}$$

Evolution of PIRO in subsonic sector $\epsilon_{\mathrm{dc}} < \epsilon_{\mathrm{ph}}$ was studied experimentally in Ref. 10, where the differential resistivity $r_{xx} = \partial E/\partial j_x \simeq \rho_H^2 \partial j_x/\partial E$ was measured. The PIRO contribution to the differential resistivity $r_{xx}^{(\mathrm{osc})}$ can be evaluated using Eqs. (4) and (5) as $r_{xx}^{(\mathrm{osc})}/\rho_D = \partial/\partial\epsilon_{\mathrm{dc}}[\epsilon_{\mathrm{dc}}\Gamma_{\mathrm{ph}}^{(\mathrm{osc})}(\epsilon_{\mathrm{dc}},\epsilon_{\mathrm{ph}})]$.

In Fig. 2 we plot $r_{xx}^{(\mathrm{osc})}$, calculated according to Eqs. (3) and (6) with $\tau_q = 8$ ps as a function of $B = B_0/\epsilon_{\mathrm{ph}}$ for several values of the total current $I = j_x w = I_0\epsilon_{\mathrm{dc}}/\epsilon_{\mathrm{ph}}$. Here $w = 50$ μm is the Hall bar width, $B_0 = 2p_F smc/e = 7.67$ kG and $I_0 = eN_e sw = 223$ μA are the reference field and current; values of the parameters s, N_e, and w were taken from Ref. 10. This theoretical result quantitatively reproduces the experimentally observed evolution of PIRO with increasing I (Ref. 10) without fitting parameters. In qualitative agreement with Ref. 10, similar oscillations with $\epsilon_{\mathrm{ph}} - \epsilon_{\mathrm{dc}}$ were obtained numerically using balance-equation approach in Ref. 19.

The important feature of Eq. (9) is the change in the phase of oscillations across the sound barrier $v_H = s$ [see Fig. 1(c)], which calls for an experimental verification. In the supersonic sector $\epsilon_{\mathrm{dc}} > \epsilon_{\mathrm{ph}}$, see Fig. 1(d), the scattering along electric field always results in gain in the Landau-level index while scattering against electric field reduces the Landau-level index.

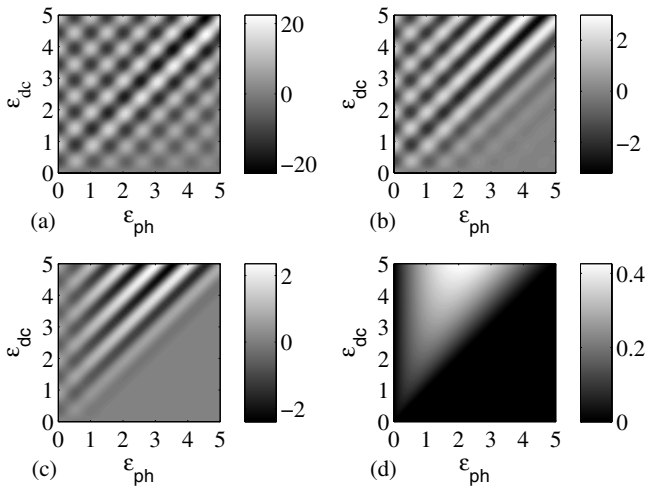

FIG. 3. [(a)–(c)] Oscillatory part of the phonon-assisted differential resistivity $r_{xx}^{(\mathrm{osc})}$ in units $2\lambda^2 g^2 \rho_D \omega_c \tau_{\mathrm{tr}}$ calculated using Eqs. (4) and (5) for the case of high [$T = 5\omega_c$, panel (a)], intermediate [$T = 0.7\omega_c$, panel (b)], and low [$T = 0.25\omega_c$, panel (c)] temperature. Panel (d): smooth part of phonon-assisted scattering rate $\Gamma_{\mathrm{ph}}^{(\mathrm{sm})}(\epsilon_{\mathrm{dc}},\epsilon_{\mathrm{ph}})$ at zero temperature, measured in units of $g^2\omega_c$, Eq. (14).

In the extreme limit of strong B or soft phonons $\epsilon_{\mathrm{ph}} \ll 1$ [see region (e) in Fig. 1(e)], Eq. (6) gives

$$\frac{\Gamma_{\mathrm{ph}}^{(\mathrm{osc})}(\epsilon_{\mathrm{dc}},0)}{2\lambda^2 g^2 T} \approx J_0^2(\pi\epsilon_{\mathrm{dc}}) - J_1^2(\pi\epsilon_{\mathrm{dc}}) - J_0(\pi\epsilon_{\mathrm{dc}})J_2(\pi\epsilon_{\mathrm{dc}}). \tag{10}$$

Here, the electron-phonon scattering behaves as a scattering off nearly static impurities and the functional form Eq. (10) coincides with that of HIRO, presented above as $F''(\pi\epsilon_{\mathrm{dc}})$, for the specific case of isotropic disorder scattering, $\tau_\theta \equiv \tau_0$.

At lower temperatures T, the phonon-assisted magneto-oscillations in differential resistivity become suppressed completely in the subsonic regime. However, in the supersonic regime only ϵ_+ oscillations vanish while amplitude of ϵ_- oscillations saturates, see Figs. 3(a)–3(c).

This behavior can also be inferred from the analytical results for $\Gamma_{\mathrm{ph}}^{(\mathrm{osc})}$, Eq. (5), obtained for low temperatures $T \lesssim 2p_F s$ but still $T \gtrsim \omega_c$. For $\epsilon_{\mathrm{dc}} < \epsilon_{\mathrm{ph}}$, we have

$$\Gamma_{\mathrm{ph}}^{(\mathrm{osc})}(\epsilon_{\mathrm{dc}},\epsilon_{\mathrm{ph}}) = \frac{4\lambda^2 g^2 \omega_c \epsilon_{\mathrm{ph}}}{\pi^2 \epsilon_{\mathrm{dc}}^{3/2}} \exp(-2|\epsilon_-|\omega_c/T) \times [\sqrt{|\epsilon_-|}\cos 2\pi\epsilon_- + \sqrt{\epsilon_+} e^{-2\epsilon_{\mathrm{dc}}\omega_c/T} \sin 2\pi\epsilon_+]. \tag{11}$$

$\Gamma_{\mathrm{ph}}^{(\mathrm{osc})}$ is exponentially small for $\epsilon_- < 0$, but as the sound barrier is reached, a nonexponential contribution emerges,

$$\Gamma_{\mathrm{ph}}^{(\mathrm{osc})}(\epsilon_{\mathrm{dc}},\epsilon_{\mathrm{ph}}) = 2\lambda^2 g^2 \omega_c \left[\frac{T/\omega_c}{3\sqrt{\pi\epsilon_{\mathrm{dc}}}\Gamma^2(3/4)} + \frac{\sqrt{8}}{\pi^2} e^{-2\epsilon_{\mathrm{dc}}\omega_c/T} \sin 4\pi\epsilon_{\mathrm{dc}}\right]. \tag{12}$$

In the supersonic regime, $\epsilon_- = \epsilon_{\mathrm{dc}} - \epsilon_{\mathrm{ph}} > 0$, we obtain

$$\Gamma_{\rm ph}^{(\rm osc)}(\epsilon_{\rm dc},\epsilon_{\rm ph}) = \frac{2\lambda^2 g^2 \omega_c \epsilon_{\rm ph}}{\pi^2 \epsilon_{\rm dc}^{3/2}} \times [\sqrt{\epsilon_-}\sin 2\pi\epsilon_- + \sqrt{\epsilon_+} e^{-2\epsilon_{\rm ph}\omega_c/T} \sin 2\pi\epsilon_+]. \quad (13)$$

A similar behavior also occurs with the smooth component of the electron-phonon rate $\Gamma_{\rm ph}^{(\rm sm)}$: it vanishes in the subsonic regime and saturates in the supersonic regime, see Fig. 3(d). For $T=0$, the smooth component,

$$\Gamma_{\rm ph}^{(\rm sm)}(\epsilon_{\rm dc},\epsilon_{\rm ph}) = \frac{8g^2\omega_c\epsilon_{\rm ph}}{3\pi^2}\left[\arccos\frac{\epsilon_{\rm ph}}{\epsilon_{\rm dc}} - \frac{\epsilon_{\rm ph}}{\epsilon_{\rm dc}^2}\sqrt{\epsilon_+\epsilon_-}\right] \quad (14)$$

for $\epsilon_{\rm dc} > \epsilon_{\rm ph}$ and $\Gamma_{\rm ph}^{(\rm sm)}(\epsilon_{\rm dc},\epsilon_{\rm ph})=0$ otherwise. At finite but low temperature, $\Gamma_{\rm ph}^{(\rm sm)}(\epsilon_{\rm dc},\epsilon_{\rm ph})$ remains small in the subsonic sector and grows continuously across the sound barrier.

Such contrast in low-temperature behavior of electron-phonon-scattering rates $\Gamma_{\rm ph}^{(\rm sm)}$ and $\Gamma_{\rm ph}^{(\rm osc)}$ in the subsonic and supersonic regimes can be understood from the structure of Eq. (2). At low temperatures $T \lesssim 2p_F s$, the occupation number of phonon modes with energy $\omega \sim 2p_F s$ is exponentially small. Therefore, the electron scattering off thermal phonons becomes negligible. At the same time, the spontaneous emission of phonons depends only on the combination $f(\varepsilon_{in})[1-f(\varepsilon_f)]$ of electron occupation numbers $f(\varepsilon)$ at initial (ε_{in}) and final (ε_f) energies. For emission processes, this combination is also exponentially small in equilibrium, but may remain finite in a system subject to electric fields. When the Hall drift exceeds the speed of sound, ε_f for electron scattering with increase in electrostatic energy is larger than ε_i even for the process with phonon emissions, see Fig. 1(d), and the spontaneous phonon emission takes place.

We developed a theory of phonon-assisted magneto-oscillations in strong dc electric fields. In the limit of a weak Hall field, $\epsilon_{\rm dc} \ll 1 \ll \epsilon_{\rm ph}$, or in the limit of quasielastic phonon scattering, $\epsilon_{\rm ph} \ll 1 \ll \epsilon_{\rm dc}$, the theory is consistent with the known results for PIRO (Ref. 18) and HIRO.[7] In the nonlinear dc response $\epsilon_{\rm dc} < \epsilon_{\rm ph}$, the theory reproduces the evolution of PIRO observed in recent experiment, cf. Ref. 10 and Fig. 2. We find that the phase of oscillations changes across the sound barrier at $\epsilon_{\rm dc}=\epsilon_{\rm ph}$, where the Hall drift velocity $v_H = cE/B$ reaches the speed of sound s, which also warrants an experimental verification. In the supersonic regime $\epsilon_{\rm dc} > \epsilon_{\rm ph}$, the amplitude of oscillations saturates at finite value for very low temperatures $T \ll \omega_\pi$, while in the subsonic sector $\epsilon_{\rm dc} < \epsilon_{\rm ph}$ the phonon-assisted current decays exponentially with lowering T, as the number of thermal phonons decreases. At zero temperature, the smooth part of the phonon-assisted nonlinear conductivity also exhibits saturation to a finite value in the supersonic regime while vanishes in the subsonic regime.

We gratefully acknowledge D. N. Aristov, A. A. Bykov, M. Khodas, A. J. Millis, A. D. Mirlin, D. G. Polyakov, I. V. Protopopov, S. A. Vitkalov, and M. A. Zudov for discussions. I.D. was supported by the DFG, by the DFG-CFN, by Rosnauka Grant No. 02.740.11.5072, by the RFBR, and M.V. was supported by NSF under Grant No. DMR-0955500.

*Also at Ioffe Physical Technical Institute, 194021 St. Petersburg, Russia.

†Present address: Institute of Mechanics, University of Kassel, 34125 Kassel, Germany.

[1] M. A. Zudov *et al.*, Phys. Rev. B **64**, 201311(R) (2001); P. D. Ye *et al.*, Appl. Phys. Lett. **79**, 2193 (2001).

[2] A. C. Durst *et al.*, Phys. Rev. Lett. **91**, 086803 (2003); I. A. Dmitriev *et al.*, *ibid.* **91**, 226802 (2003); X. L. Lei *et al.*, *ibid.* **91**, 226805 (2003); M. G. Vavilov *et al.*, Phys. Rev. B **69**, 035303 (2004); I. A. Dmitriev *et al.*, *ibid.* **71**, 115316 (2005); J. Dietel *et al.*, *ibid.* **71**, 045329 (2005); I. A. Dmitriev *et al.*, *ibid.* **75**, 245320 (2007); I. A. Dmitriev *et al.*, *ibid.* **80**, 165327 (2009).

[3] V. I. Ryzhii, Sov. Phys. Solid State **11**, 2078 (1970); V. I. Ryzhii *et al.*, Sov. Phys. Semicond. **20**, 1299 (1986).

[4] R. G. Mani *et al.*, Nature (London) **420**, 646 (2002); M. A. Zudov *et al.*, Phys. Rev. Lett. **90**, 046807 (2003); C. L. Yang *et al.*, *ibid.* **91**, 096803 (2003); R. L. Willett *et al.*, *ibid.* **93**, 026804 (2004); J. H. Smet *et al.*, *ibid.* **95**, 116804 (2005); M. A. Zudov *et al.*, Phys. Rev. B **73**, 041303(R) (2006); C. L. Yang *et al.*, *ibid.* **74**, 045315 (2006); A. A. Bykov *et al.*, JETP Lett. **84**, 391 (2006).

[5] A. V. Andreev *et al.*, Phys. Rev. Lett. **91**, 056803 (2003); J. Shi *et al.*, *ibid.* **91**, 086801 (2003); A. Auerbach *et al.*, *ibid.* **94**, 196801 (2005).

[6] C. L. Yang *et al.*, Phys. Rev. Lett. **89**, 076801 (2002); A. A. Bykov *et al.*, Phys. Rev. B **72**, 245307 (2005); W. Zhang *et al.*, *ibid.* **75**, 041304(R) (2007); A. T. Hatke *et al.*, *ibid.* **79**, 161308(R) (2009); S. Vitkalov, Int. J. Mod. Phys. B **23**, 4727 (2009).

[7] M. G. Vavilov *et al.*, Phys. Rev. B **76**, 115331 (2007).

[8] A. A. Bykov *et al.*, Phys. Rev. Lett. **99**, 116801 (2007); A. T. Hatke *et al.*, Phys. Rev. B **82**, 041304(R) (2010).

[9] M. A. Zudov *et al.*, Phys. Rev. Lett. **86**, 3614 (2001); A. A. Bykov *et al.*, JETP Lett. **81**, 523 (2005).

[10] W. Zhang *et al.*, Phys. Rev. Lett. **100**, 036805 (2008).

[11] A. T. Hatke *et al.*, Phys. Rev. Lett. **102**, 086808 (2009).

[12] A. A. Bykov *et al.*, Phys. Rev. B **81**, 155322 (2010).

[13] A. T. Hatke *et al.*, Phys. Rev. B **77**, 201304(R) (2008).

[14] M. Khodas *et al.*, Phys. Rev. B **78**, 245319 (2008).

[15] M. Khodas *et al.*, Phys. Rev. Lett. **104**, 206801 (2010).

[16] I. A. Dmitriev *et al.*, Phys. Rev. B **80**, 125418 (2009).

[17] We consider interaction with 2D isotropic deformational phonons justified if z component of relevant phonon momentum is negligible (i.e., the width of the quantum well where 2DEG is confined $b \gg k_F^{-1}, s/T$). In this case, $g^2 = mD^2/\rho b s^2$ in terms of the mass density ρ and deformation potential D of the host crystal.

[18] O. E. Raichev, Phys. Rev. B **80**, 075318 (2009).

[19] X. L. Lei, Phys. Rev. B **77**, 205309 (2008).